



1

2 **Summer fluxes of methane and carbon dioxide from a pond**
3 **and floating mat in a continental Canadian peatland**

4

5 **M. Burger^{1,2}, S. Berger^{1,2}, I. Spangenberg^{1,2} and C. Blodau^{1,2}**

6 [1] Ecohydrology and Biogeochemistry Group, Institute of Landscape Ecology, University of
7 Münster, Germany

8 [2] School of Environmental Sciences, University of Guelph, Canada

9 *Correspondence to:* C. Blodau (christian.blodau@uni-muenster.de)

10 **Abstract**

11 Ponds smaller than 10000 m² likely account for about one third of the global lake perimeter.
12 The release of methane (CH₄) and carbon dioxide (CO₂) from these ponds is often high and
13 significant on the landscape scale. We measured CO₂ and CH₄ fluxes in a temperate peatland
14 in southern Ontario, Canada, in summer 2014 along a transect from the open water of a small
15 pond (847 m²) towards the surrounding floating mat (5993 m²) and in a peatland reference area.
16 We used a high-frequency closed chamber technique and distinguished between diffusive and
17 ebullitive CH₄ fluxes. CH₄ fluxes and CH₄ bubble frequency increased from a median of 0.14
18 (0.00 to 0.43) mmol m⁻² h⁻¹ and 4 events m⁻² h⁻¹ on the open water to a median of 0.80 (0.20
19 to 14.97) mmol m⁻² h⁻¹ and 168 events m⁻² h⁻¹ on the floating mat. The mat was a summer hot
20 spot of CH₄ emissions. Fluxes were one order of magnitude higher than at an adjacent peatland
21 site. During daytime the pond was a net source of CO₂ equivalents to the atmosphere amounting
22 to 0.13 (−0.02 to 1.06) g CO₂ equivalents m⁻² h⁻¹, whereas the adjacent peatland site acted as a
23 sink of −0.78 (−1.54 to 0.29) g CO₂ equivalents m⁻² h⁻¹. The photosynthetic CO₂ uptake on the
24 floating mat did not counterbalance the high CH₄ emissions, which turned the floating mat into
25 a strong net source of 0.21 (−0.11 to 2.12) g CO₂ equivalents m⁻² h⁻¹. This study highlights the
26 large small-scale variability of CH₄ fluxes and CH₄ bubble frequency at the peatland-pond
27 interface and the importance of the often large ecotone areas surrounding small ponds as a
28 source of greenhouse gases to the atmosphere.



1 1. Introduction

2 Inland waters play a significant role in the global carbon cycle although covering only 3.7 % of
3 the Earth's land surface (Bastviken et al., 2011; Raymond et al., 2013; Tranvik et al., 2009).
4 They transport and sequester autochthonous and terrestrially derived carbon and are also
5 sources of carbon dioxide (CO₂) and methane (CH₄) to the atmosphere (Cole et al., 2007;
6 Tranvik et al., 2009). Global estimates of CO₂ and CH₄ emissions from inland waters have
7 recently been corrected upward to 2.1 Pg C yr⁻¹ as CO₂ (Raymond et al., 2013) and 0.65 Pg C
8 yr⁻¹ as CH₄ (Bastviken et al., 2011). Together they are similar to the net carbon uptake by
9 terrestrial ecosystems of -2.5 ± 1.3 Pg C yr⁻¹ and to approximately one third of the
10 anthropogenic CO₂ emissions (Ciais et al., 2013).

11 Small aquatic systems may be particularly important in this respect (Downing, 2010).
12 According to high-resolution satellite imagery analyzed by Verpoorter et al. (2014), 77 % of
13 the total 117 million lakes belong to the smallest detectable size category of 2000 to 10000 m²
14 lake area. These waters only contribute 7 % to the area but 32 % to the total lake perimeter
15 (Verpoorter et al., 2014). Numerous processes were found to proceed faster in small aquatic
16 systems than in larger ones. Sequestration rates of organic carbon (Downing, 2010; Downing
17 et al., 2008), the concentrations of CH₄, CO₂, and dissolved organic carbon (DOC) in the water
18 column (Bastviken et al., 2004; Juutinen et al., 2009; Kelly et al., 2001; Kortelainen et al., 2006;
19 Xenopoulos et al., 2003), and CH₄ and CO₂ emissions from the water to the atmosphere increase
20 with decreasing lake size (Juutinen et al., 2009; Kortelainen et al., 2006; Michmerhuizen et al.,
21 1996; Repo et al., 2007).

22 Small and shallow lakes and ponds are common in flat northern glacial landscapes and abundant
23 in peatland areas, where 20 to 30 % of the world's soil organic carbon is stored (Turunen et al.,
24 2002). CO₂ emissions from peatland ponds were reported to be in the same order of magnitude
25 than net uptake of CO₂ by the peatland vegetation (Dinsmore et al., 2009; Hamilton et al., 1994).
26 CH₄ emissions from open waters generally exceed CH₄ fluxes from vegetated areas by a factor
27 3 to 25 (Hamilton et al., 1994; McLaughlin and Webster, 2014; Trudeau et al., 2013). Moreover,
28 CH₄ and CO₂ emissions from open waters can be significant on the landscape scale despite their
29 often small area (Dinsmore et al., 2010; Juutinen et al., 2013). Pelletier et al. (2014) estimated
30 that a pond cover of > 37 % could convert a northern peatland from a carbon sink into a carbon
31 source. Such findings are relevant as Hamilton et al. (1994) and Trudeau et al. (2013) reported
32 a pond cover of 8 to 12 % and 42 % in fens and bogs in northern Canada. The authors suspected
33 a contribution of aquatic CH₄ fluxes to landscape CH₄ fluxes of 30 % and 79 %, respectively.
34 Very high CH₄ emissions have also been reported from a floating mat on a thermokarst pond
35 and a floating mat within a bog pond (Flessa et al., 2008; Sugimoto and Fujita, 1997). Juutinen



1 et al. (2013) documented highest CH₄ fluxes from a wet lawn adjacent to a small fen lake
2 compared to the lake itself and fen lawns farther away from the small lake.
3 Fluxes of CH₄ and CO₂ from ponds are controlled by environmental and biotic factors.
4 Atmospheric CH₄ fluxes are controlled by microbial production and oxidation of CH₄ within
5 peat, sediment and surface water and the diffusive, ebullitive, and plant-mediated transport to
6 the atmosphere (Bastviken et al., 2004; Bridgham et al., 2013; Carmichael et al., 2014). CO₂
7 exchange is driven by the interplay of heterotrophic and autotrophic respiration and by
8 photosynthesis of aquatic macrophytes and algae. Both gas fluxes are linked to the quantity and
9 quality of organic and inorganic carbon supplied from the surrounding catchment (Huttunen et
10 al., 2002; Macrae et al., 2004; Tranvik et al., 2009). They are also related to temperature, wind
11 speed and air pressure (e. g. Trudeau et al., 2013; Varadharajan and Hemond, 2012; Wik et al.,
12 2013). Ebullition appears to be of particular importance for CH₄ release to the atmosphere
13 (Walter et al., 2006; Wik et al., 2013) and varies on scales of several tens to hundreds of meters
14 (Bastviken et al., 2004; Wik et al., 2013). Emissions of CH₄ emissions are generally lower in
15 the pelagic than in the littoral zone, where plant habitats further influence fluxes (Juutinen et
16 al., 2001; Larmola et al., 2004). On the other hand, Trudeau et al. (2013) found 2.5 to 5 times
17 lower CH₄ fluxes at the border of fen pools than in the center of the pools with areas of 60 and
18 200 m².
19 Despite this progress, knowledge on the temporal and spatial variability of CH₄ and CO₂ fluxes
20 within small pond systems is limited. We know, for example, little about the CH₄ and CO₂
21 exchange of transition zones between ponds and surrounding peatlands, which can be especially
22 important due to the high perimeter to area ratio of small ponds (Verpoorter et al., 2014). It is
23 important to consider the net effect of different microforms of peatlands by taking into account
24 the global warming potentials, as CH₄ emissions may easily offset carbon sinks in ponds. To
25 gain more insight into these issues we investigated the summer atmospheric CO₂ and CH₄
26 exchange of open water, a floating mat and an adjacent peatland area in a temperate peatland
27 in southern Ontario, Canada. In particular we tested the hypothesis that (I) ebullitive and
28 diffusive CH₄ fluxes increase from the open water towards a floating mat surrounding the pond.
29 We examined (II) if CH₄ and CO₂ effluxes from the system increases with temperature and
30 wind speed and investigated if falling air pressure raises CH₄ fluxes. To assess the importance
31 of the pond system for the greenhouse gas balance we calculated the net radiative forcing of the
32 investigated peatland microforms.



1 2 **Materials and methods**

2 **2.1 Study site**

3 Wylde Lake Bog is located in the southeastern part of the Luther Marsh Wildlife Management
4 Area (43°54.667' N, 80°24.022' W) (Fig. 1) at about 490 m above sea level and has an area of
5 approximately 7.8 km². A 600 cm deep profile analyzed by Givelet et al. (2003) documented
6 clay-rich sediments up to 560 cm depth, gyttja from 560 to 490 cm, fen peat from 490 to
7 approximately 300 cm and bog peat above 300 cm depth. The peatland is dominated by mosses,
8 graminoids, dwarf shrubs and sporadic trees, and a pronounced hummock-hollow-
9 microtopography. Common in the peatland are *Sphagnum magellanicum*, *S. capillifolium*,
10 *Carex disperma* and *Chamaedaphne calyculata* and on the floating mat *S. angustifolium*, *S.*
11 *magellanicum* and *Rhynchospora alba*. The plant species composition of the study site is given
12 in the Supplementary Information (Table S1). The vicinity of the pond is characterized by
13 small open and larger treed areas dominated by *Larix laricina* and *Picea mariana*. The pond
14 (Fig. 1) has an area of 847 m² and a depth of 0.3 to 0.8 m. The interface between the water
15 column and the organic deposits is not clearly delimited but consists of a transition zone with
16 suspended organic material. It likely has changed in size, depth, and shape throughout the last
17 decades. Sandilands (1984) reported that larger, adjacent Wylde Lake shrunk from 0.4 km² in
18 1928 to 0.05 km² in 1984. The floating mat (Fig. 1) surrounding the pond has an area of approx.
19 5993 m². Climate is temperate continental with a mean annual air temperature of about 6.7 °C,
20 annual precipitation of 946 mm including 148 mm of snowfall, and an average frost-free period
21 from May 7th to October 6th (1981 to 2010, Fergus Shand Dam, National Climate Data and
22 Information Archive, 2014).

23

24 **2.2 Environmental variables**

25 Air temperature, relative humidity, wind speed, wind direction, photosynthetically active
26 radiation (PAR) and precipitation were recorded at the study site by a HOBO U30 weather
27 station (U30-NRC-SYS-B, Onset) (Supplementary Information, Table S2). Water temperature
28 of the pond and the temperature of the floating mat were also continuously measured. Air
29 pressure was recorded at a distance of 1.1 km from the study site (Supplementary Information,
30 Table S2).

31

32 **2.3 CH₄ and CO₂ flux measurements with closed chambers**

33 CH₄ and CO₂ fluxes of the pond and the floating mat were measured once a week from July
34 10th to September 29th, 2014 between 1 pm ± 1.5 hours and 5 pm ± 1.5 hours using closed
35 chambers designed according to Drösler (2005). The cylindrical, transparent Plexiglas



1 chambers had a basal area of 0.12 m² and a height of 0.40 m. They were equipped with 2 or 3
2 fans (Micronel Ventilator D341T012GK-2, BEDEK GmbH) to circulate the air, a
3 photosynthetically active radiation and an air temperature sensor (Supplementary Information,
4 Table S2). To compensate for air pressure differences, we attached a vent tube, 12 cm long and
5 7 mm inner diameter, to the chamber (Davidson et al., 2002). Transparent chambers were used
6 to measure net ecosystem exchange (NEE) and cooled with up to 6 ice packs depending on
7 ambient temperature to ensure a temperature change of less than 1°C during the chamber
8 closure. Ecosystem respiration (ER) was measured with chambers covered with reflective
9 insolation foil. On the water, chambers were operated with a Styrofoam float (0.80 m × 0.61 m
10 × 0.08 m). The chamber walls extended 10 cm below the water surface as recommended by
11 Soumis et al. (2008). CH₄ and CO₂ concentrations were quantified with an Ultraportable
12 Greenhouse Gas Analyzer (915-001, Los Gatos Research) at a temporal resolution of 1 s.
13 According to the manufacturer, a single data point has a precision of < 2 ppb for CH₄ and
14 < 300 ppb for CO₂. Stability of the calibration was checked in March and August 2014. The air
15 was circulated between the chamber and the analyzer through low-density polyethylene tubes
16 of 5 m length with an inner diameter of 2 mm and a water vapor trap. Using this setup it took
17 36 s until the sampling cell of the analyzer was fully flushed and the concentration had
18 stabilized.

19 Flux measurements on the open water were carried out in 6 locations with increasing distance
20 of 0.7 m to 4.6 m to the floating mat (Supplementary Information, Table S3). On the floating
21 mat the chambers were placed on cylindrical PVC collars with a height of 25 cm. Collars had
22 been inserted into the mat to depths of approximately 15 cm prior to the first measurement.
23 Each sampling day fluxes were measured at least once with the transparent and with the
24 radiation-shielded chamber, for 5 min on the pond and 3 min on the floating mat, by placing
25 the chamber gently as soon as the concentration reading was stable. When CH₄ concentrations
26 increased sharply within the first 60 s of the measurement due to CH₄ bubble release caused by
27 the positioning of the chamber, the measurement was discarded and repeated. Fluxes were also
28 quantified at a peatland site in the north-northeast of the pond (Fig. 1) with the same approach,
29 every other week from July 4th until October 1st, 2014, on 12 measuring plots covering
30 hummocks, hollows and lawns. In this area of the peatland, hummocks cover 90 % of the area,
31 hollows 9.8 % and lawns 0.2 % of the area.

32 Fluxes were calculated based on the gas concentration change in the chamber over time using
33 linear regression and the ideal gas law, mean air temperature inside the chamber and the
34 corresponding half hour mean air pressure. The chamber volume was calculated for each
35 measurement depending on the number of ice packs, immersion depth on the pond and mean
36 vegetation height on the floating mat. The first 40 s after chamber deployment were discarded



1 for flux calculation due to the response time of the concentration measurement. If the slope was
2 not significantly different from 0 (F test, $\alpha = 0.05$), the flux was set to 0. Concentration change
3 over time was only < 3 ppm CO₂ and < 0.1 ppm CH₄ in 12 % of flux measurements. These
4 measurements resulted in fluxes close to 0 with $R^2 < 0.8$. Following Repo et al. (2007), we
5 included them in the data set because their exclusion would have biased the results by increasing
6 the median diffusive fluxes by 52 % (CO₂) and 12 % (CH₄).

7 Due to the high temporal resolution of concentration measurements, we were able to quantify
8 CH₄ fluxes with and without bubbles. When the CH₄ concentrations evolved linearly with a
9 constant slope we used linear regression over the entire time of sampling; when the initial
10 concentration trend was interrupted by one or several sharp increases in slope, followed by a
11 return to the initial slope (Supplementary Information, Fig. S1), we used piecewise linear fitting
12 for each of the linear segments (Goodrich et al., 2011). According to Goodrich et al. (2011) and
13 Xiao et al. (2014), we define sharp increases in slope as ebullitive CH₄ fluxes and all others as
14 diffusive or continuous flux of micro-bubbles. Time-weighted averages including diffusive and
15 ebullitive flux segments were calculated. We also computed the CH₄ bubble frequency in events
16 $\text{m}^{-2} \text{h}^{-1}$ as the number of bubble events divided by measuring time and area. In order to evaluate
17 the contribution of ebullitive CH₄ flux to the total CH₄ flux, the CH₄ release of each event in
18 μmol was calculated by multiplying the ebullitive flux with the duration of the event and the
19 basal area of the chamber.

20 For comparisons of NEE between sites and with time, we used the maximum NEE defined as
21 light-saturated at PAR levels $> 1000 \mu\text{mol m}^{-2} \text{s}^{-1}$ according to a study by Larmola et al. (2013).
22 We further calculated the net exchange of CO₂ equivalents for each flux measurement. To this
23 end, the CH₄ flux was converted into CO₂ equivalents by multiplying the mass flux with the
24 global warming potential of 28 for a 100 year time horizon (Myhre et al., 2013). Subsequently,
25 the CH₄ flux in CO₂ equivalents and the maximum NEE were summed up.

26

27 **2.4 CO₂ concentration measurements and gradient flux calculations**

28 Concentrations of CO₂ in the surface water of the pond and in the air were measured with
29 calibrated non-dispersive infrared absorption sensors (CARBOCAB, GMP222, Vaisala) in the
30 range up to 10000 ppm and with an accuracy of ± 150 ppm plus 2 % of the reading. The probe
31 was enclosed in CO₂ permeable silicone tubes, as already used by Estop et al. (2012) in peats,
32 and attached to a floating platform at a depth of approximately 18 cm and a distance of 3.2 m
33 from the pond margin. In water equilibration time to 90% of dissolved concentration was
34 approximately one hour when concentration increased but more delayed when it fell
35 (Supplementary Information, Figure S3). The platform also carried the data logger (MI70,
36 Vaisala). Another silicon-covered sensor measured air CO₂ concentrations at 0.3 m above the



1 water surface. Concentration was recorded every 15 min and CO₂ flux across the air-water
2 interface estimated according to the boundary layer equation approach (Supplementary
3 Information). Due to frequent failures of the sensors with increased humidity in the sensor head
4 and overheating of the data logger, CO₂ fluxes were only calculated for 5 and 3 exemplary days
5 in July and September, respectively. During these periods sensor functioning was stable.
6

7 **2.5 CH₄ and CO₂ concentrations and diffusive fluxes in the sediment**

8 Dissolved CH₄ and CO₂ concentrations at the sediment-water-interface were determined with
9 pore water peepers of 60 cm length and 1 cm resolution as developed by Hesslein (1976). The
10 chambers were filled with deionized water, covered with a nylon membrane of 0.2 μm pore
11 size, installed at four locations in the pond on August 21st, 2014 and sampled on September 25th
12 and 29th, 2014. The pH of every other cell was measured in the field and a sample of 0.5 mL
13 from each chamber filled into a vial containing 20 μL of 4 M hydrochloric acid (HCl). CO₂ and
14 CH₄ concentrations in the headspace of the vials were determined with an SRI 8610C gas
15 chromatograph equipped with a methanizer and a flame ionization detector on the day after
16 sampling. The original CO₂ and CH₄ concentrations in the pore water were calculated by using
17 the measured headspace concentrations, Henry's law with temperature corrected Henry's law
18 constants (Sander, 1999) and the ideal gas law. Diffusive fluxes of CO₂ and CH₄ towards the
19 sediment-water interface were calculated with Fick's first law and diffusion coefficients in
20 water D_w corrected for an assumed sediment temperature of 15°C (CH₄: 1.67 • 10⁻⁵ cm² s⁻¹;
21 CO₂: 1.87 • 10⁻⁵ cm² s⁻¹) and assuming a porosity n of 0.9. The effect of porosity on the sediment
22 diffusion coefficient was accounted for by multiplying D_w with a factor n² (Lerman, 1978). We
23 further calculated a theoretical temperature- and depth-dependent threshold of bubble formation
24 using Henry's law, correcting Henry's law constant for a temperature of 15°C, and assuming a
25 partial pressure of N₂ in the pore water of 0.8 atm or 0.5 atm. The assumption here is that bubble
26 formation is possible when the partial pressure of CH₄ and remaining N₂ exceeds atmospheric
27 and water pressure in the anoxic sediment.
28

29 **2.6 Statistical analyses**

30 Statistical analyses were performed with R, version 3.1.2 (R Core Team, 2014). All datasets
31 were checked for normality with the Shapiro-Wilk normality test at a confidence level of
32 $\alpha = 0.05$. To investigate statistical differences of a continuous variable between two or more
33 groups, we used the non-parametric Kruskal-Wallis rank sum test ($\alpha = 0.05$) and if applicable
34 afterwards the multiple comparison test after Kruskal-Wallis ($\alpha = 0.05$) since none of the
35 datasets were normally distributed. For the investigation of relationships between two
36 continuous variables, we used Spearman's rank correlation ($\alpha = 0.05$). Due to visually different



1 dynamics of the gas fluxes from July 10th to August 7th (here called “mid summer”) compared
2 to August 15th to September 29th (here called “late summer”), correlations with environmental
3 variables were examined for the whole period as well as the two subperiods.

4

5

6 **3 Results**

7 **3.1 Weather conditions**

8 Three distinct periods of weather occurred. From July 10th until September 10th, 2014, air
9 temperatures remained high with a mean (\pm standard deviation) of 17.0 ± 2.7 °C (Fig. 2). Most
10 days were sunny with some passing clouds. From September 11th to September 22nd, 2014,
11 mean air temperature had cooled to 10.2 ± 2.8 °C and the first frost occurred on September 14th
12 (Fig. 2). From September 23rd to 29th, mean air temperature was 13.2 ± 7.6 °C with a high daily
13 amplitude from 3.7 ± 1.3 °C to 24.3 ± 1.5 °C and wind speed was low with a mean of $0.14 \pm$
14 0.31 m s⁻¹ (5 min averages) (Fig. 2). Major storms with maximum wind speeds from 3 to 5.5
15 m s⁻¹ on July 23rd, July 28th, August 12th, September 6th, September 11th and September 21st
16 were accompanied by air pressure decline to minima between 944 and 955 hPa. Often rainfall
17 reached an intensity of 2.8 to 6.2 mm in the chosen 5 min time intervals (Fig. 2).

18

19 **3.2 CH₄ and CO₂ fluxes over time**

20 CH₄ fluxes from the pond were significantly lower in the period from July 10th until August 7th
21 with a median of 0.03 mmol m⁻² h⁻¹ compared to a median of 0.21 mmol m⁻² h⁻¹ from August
22 15th until September 29th (Kruskal-Wallis test, $p < 0.001$, $n = 159$) (Fig. 3 A). The highest
23 median CH₄ flux, highest maximum flux, and largest variability were observed on August 15th.
24 The bubble frequency varied between 0 and 30 events m⁻² h⁻¹ (Fig. 3 B) and the contribution
25 of the ebullitive to the total CH₄ flux between 90 % on July 22nd and 0 % on September 17th,
26 25th and 29th (Fig. 3 C). Efflux of CH₄ from the floating mat was variable but significantly
27 higher from August 15th to September 29th with a median of 0.80 mmol m⁻² h⁻¹ than in the
28 period from July 10th to August 7th with a median of 0.22 mmol m⁻² h⁻¹ (Kruskal-Wallis test,
29 $p < 0.001$, $n = 84$) (Fig. 4 A). The bubble frequency on the floating mat ranged from 0 to 80
30 events m⁻² h⁻¹ and the contribution of ebullition to CH₄ flux from 0 to 88 % (Fig. 4 B and C).
31 At the peatland site, CH₄ fluxes were similar over time with a median of 0.31 mmol m⁻² h⁻¹
32 and two very high individual fluxes on September 1st and October 1st (Fig. 5 A). The bubble
33 frequency and contribution of ebullition to CH₄ flux ranged from 0 to 5 events m⁻² h⁻¹ and 0 to
34 54 %, respectively (Fig. 5 B and C).



1 CO₂ fluxes from the pond from July 10th until August 7th had a median of 0.11 mmol m⁻² h⁻¹
2 and were also significantly lower than the pond CO₂ fluxes from August 15th until September
3 29th with a median of 1.80 mmol m⁻² h⁻¹ (Kruskal-Wallis test, $p < 0.001$, $n = 159$) (Fig. 3 D).
4 During 24 out of 55 individual measurements before August 15th, CO₂ exchange across the
5 water-atmosphere interface was absent or CO₂ was taken up by the pond between 0 and
6 -0.75 mmol m⁻² h⁻¹. From August 15th on CO₂ was net emitted. The median daytime ER of the
7 floating mat was 6.77 mmol m⁻² h⁻¹ and the median of the maximum NEE -4.81 mmol m⁻² h⁻¹
8 (Fig. 4 D). Daytime ER at the peatland site varied between 2.61 to 36.93 mmol m⁻² h⁻¹ with a
9 median of 11.98 mmol m⁻² h⁻¹ and tended to decrease towards fall (Fig. 5 D). The maximum
10 NEE was quite constant from July until September with a median of -16.98 mmol m⁻² h⁻¹.
11 The gradient method provided similar CO₂ fluxes in July and September with a median of
12 1.99 mmol m⁻² h⁻¹ in July and 2.02 mmol m⁻² h⁻¹ in September (Supplementary Information,
13 Fig. S2). The daily amplitude of fluxes was 1.46 to 3.19 mmol m⁻² h⁻¹ in July and 1.41 to
14 1.86 mmol m⁻² h⁻¹ in September (Supplementary Information Fig. S2). In July, however, the
15 daytime CO₂ fluxes obtained by the gradient method were 14-fold higher than the respective
16 CO₂ fluxes measured with the floating chambers (Kruskal-Wallis test, $p < 0.001$, $n = 189$). No
17 significant differences occurred between the methods in September.

18

19 3.3 CO₂ and CH₄ concentrations and diffusion in the surface water and sediments

20 CO₂ concentrations of the surface water of the pond were similar during the examined periods
21 in July and September with a mean (\pm standard deviation) of 114.8 ± 33.1 $\mu\text{mol L}^{-1}$ and 132.0
22 ± 21.0 $\mu\text{mol L}^{-1}$, respectively (Fig. S2, Supplementary Information). In both periods we
23 observed diurnal cycles of CO₂ concentrations covering a mean amplitude of 83.5 ± 16.3
24 $\mu\text{mol L}^{-1}$ (July) and 62.0 ± 3.1 $\mu\text{mol L}^{-1}$ (September). In the sediments, the mean pH was 4.29
25 ± 0.11 above the sediment-water interface and increased to 5.37 ± 0.28 at a sediment depth of
26 40 to 60 cm. CH₄ concentrations rose with depth from an average of 10.7 ± 20.4 $\mu\text{mol L}^{-1}$ above
27 the sediment-water interface to 557.3 ± 72.9 $\mu\text{mol L}^{-1}$ at a depth of 40 to 60 cm into the
28 sediment (Fig. 6). The concentration began exceeding theoretical thresholds for bubble
29 formation at depths between 10 to 40 cm and at a partial pressure of N₂ of 0.8 atm, but nowhere
30 were concentrations sufficient to form bubbles at 0.5 atm N₂ (Fig. 6). The average CO₂
31 concentration at 40 to 60 cm depth was 1548.2 ± 332.5 $\mu\text{mol L}^{-1}$ and one order of magnitude
32 higher than above the sediment-water interface (Fig. 6). Diffusive fluxes towards the surface
33 water were on average 10.5 ± 5.6 $\mu\text{mol m}^{-2} \text{h}^{-1}$ (CH₄) and 16.9 ± 9.4 $\mu\text{mol m}^{-2} \text{h}^{-1}$ (CO₂), or 12.0
34 ± 5.6 $\mu\text{mol m}^{-2} \text{h}^{-1}$ (CH₄) and 25.8 ± 16.1 $\mu\text{mol m}^{-2} \text{h}^{-1}$, depending on where the concentration
35 gradient of pore water peeper C is assigned (Fig. 6). *In situ* production and diffusion from the
36 sediment thus contributed only a very small fraction to the CO₂ and CH₄ flux from the pond.



1 The relative inactivity of the pond sediment was also indicated by the mostly flat and linear
2 concentration increase of both gases with depth near the sediment-water interface.

3

4 **3.4 Spatial pattern of CH₄ and CO₂ fluxes**

5 Efflux of CH₄ increased 6-fold from open water towards the floating mat and was also much
6 higher on the floating mat than at the peatland site (Fig. 7 A). The open water median CH₄ flux
7 of plot p1, p2 and p3, farthest away from the floating mat, was 0.12 mmol m⁻² h⁻¹ and
8 significantly lower than from plot p4, p5 and p6 closer to the floating mat with a median of 0.19
9 mmol m⁻² h⁻¹ (Kruskal-Wallis test, $p < 0.05$, $n = 82$) (Supplementary Information, Table S3).
10 The median CH₄ flux of the floating mat was 0.64 mmol m⁻² h⁻¹ and significantly higher than
11 the CH₄ flux from the pond (Kruskal-Wallis test, $p < 0.001$, $n = 243$). We observed an increasing
12 frequency of ebullition and a higher contribution to CH₄ flux towards the floating mat. On plot
13 p1 only 4 events m⁻² h⁻¹ contributing 5 % occurred, whereas on plot m3 on the floating mat
14 168 events m⁻² h⁻¹ contributing 78 % were found (Fig. 7 B and C). The CH₄ flux of m3 was
15 significantly higher than of m1 and m2 (Kruskal-Wallis multiple comparison test, $p < 0.05$,
16 $n = 84$).

17 The frequency of ebullition and the amount of CH₄ released by bubble events differed along
18 the transect and in comparison to the peatland site. On the pond, bubble events with a
19 comparatively small CH₄ release of 0 to 2.5 μmol were most frequent and occurred 5.4 times
20 m⁻² h⁻¹ (Fig. 8). They also contributed the most to the total CH₄ release. Bubble events releasing
21 a larger amount of CH₄ were rare. The contribution of ebullition to CH₄ release was 27 %. On
22 the floating mat, CH₄ release by individual bubble events was highly variable with a maximum
23 of 50 μmol (Fig. 8). Larger bubble events were less frequent than smaller ones. However,
24 medium and larger bubble events contributed most to CH₄ release with up to 8 %. The
25 contribution of ebullition to CH₄ release was 66 % on the floating mat. In contrast, it was only
26 20 % in the peatland with a clearly different frequency distribution (Fig. 8). Bubble events
27 occurred over a larger range of release strength than on the pond, but they were less frequent
28 with a total bubble frequency of only 1.3 events m⁻² h⁻¹.

29 The pond was on average also a net source of CO₂ with a median CO₂ efflux of 1.16
30 mmol m⁻² h⁻¹ (Fig. 7 D). On the floating mat, daytime ER ranged from 0.53 to 13.45 mmol
31 m⁻² h⁻¹ and maximum NEE from -11.46 to 0.71 mmol m⁻² h⁻¹ (Fig. 7 D).

32

33 **3.5 Controls on CH₄ and CO₂ fluxes**

34 CH₄ and CO₂ fluxes from the pond and ER on the floating mat were significantly negatively,
35 and maximum NEE on the floating mat positively correlated with air, water and mat
36 temperature (Table 1 and 2). We found more negative NEE values at an increasing PAR on the



1 floating mat as well as on the pond. Late summer fluxes of CO₂ and CH₄ across the water-
2 atmosphere interface were positively correlated with wind speed, whereas the respective mid-
3 summer fluxes were negatively correlated (Table 1 and 2).

4 CH₄ fluxes from the floating mat and the pond were significantly higher for periods with a
5 decreasing air pressure trend over the last 24 h than for periods with an increasing air pressure
6 trend (Kruskal-Wallis test, $p < 0.05$ and $p < 0.01$, $n = 111$ and $n = 61$) (Fig. 9).

7

8 **3.6 Greenhouse gas exchange of the pond system compared to the surrounding peatland**

9 During our daytime measurements the pond and the floating mat were most frequently
10 significant net sources of CO₂ equivalents, whereas the peatland was generally a sink of CO₂
11 equivalents (Fig. 10; Kruskal-Wallis multiple comparison test, $p < 0.001$, $n = 218$). The source
12 strength of CO₂ equivalents was largest on the floating mat with a median of 0.21 g CO₂
13 equivalents m⁻² h⁻¹. While the floating mat and peatland site took up CO₂ at PAR > 1000 μmol
14 m⁻² s⁻¹, the pond emitted CO₂ to the atmosphere during 90 % of measurements (see Figs. 3, 4,
15 5). When both greenhouse gases were emitted, CH₄ contributed 59 ± 20 % to the total emission
16 of CO₂ equivalents of the pond.

17

18

19 **4 Discussion**

20 **4.1 Spatial pattern of CH₄ and CO₂ fluxes along the peatland – pond ecotone**

21 The peatland and especially the floating mat were summer hot spots of CH₄ emissions compared
22 to a variety of sites in other northern peatlands. Fluxes exceeded most, but not all, emissions
23 recently reported from similar environments by an order of magnitude (Supplementary
24 Information, Table S4). On a per-day and mass basis mean fluxes reached 204 and 437 mg
25 CH₄-C m⁻² d⁻¹, which is at the high end of fluxes reported in meta-analyses (Olefeldt et al.,
26 2013). Average CH₄ emissions from the open water were still substantial at 63 mg CH₄-C m⁻²
27 d⁻¹, which is about 5 times the flux reported from the multi-year study of Stordalen Mire in
28 Northern Sweden (Wik et al., 2013). Emissions fell, however, well into the range of fluxes
29 reported from other peatland ponds (Supplementary Information, Table S4). In contrast, CO₂
30 fluxes were fairly inconspicuous compared to fluxes in similar systems (see Supplementary
31 Information, Table S5, S6); on a per-day and mass basis mean maximum NEE reached -5.4 g
32 CO₂-C m⁻² d⁻¹ in the bog and -1.27 g CO₂-C m⁻² d⁻¹ on the floating mat, and daytime ER 3.91
33 g CO₂-C m⁻² d⁻¹ and 1.85 g CO₂-C m⁻² d⁻¹, respectively. The pond on average emitted 0.38 g
34 CO₂-C m⁻² d⁻¹. Both pond and floating mat thus lost more CO₂ than they fixed during the day,



1 which suggests that in both environments additional CO₂ was released, for example stemming
2 from carbon-rich groundwater seeping into the pond.
3 Part of the surprising source strength of methane can be attributed to the inclusion of ebullition
4 by means of high frequency chamber measurements, similarly as first reported by Goodrich et
5 al. (2011). Fluxes that are visibly affected by ebullition events have often been discarded from
6 static chamber fluxes in the past because the non-linearity of concentration increase over time
7 is problematic when few samples are analyzed by gas chromatography. Ebullition contributed
8 on average 66 % to the emissions on the floating mat and reached 78 % at the plot with the
9 highest methane flux (Figs. 4 and 7). The importance and variability of ebullition was similar
10 as reported from an ombrotrophic peatland in Japan (50 to 64 %; Tokida et al., 2007). The CH₄
11 released by individual bubble events from the floating mat was also on the same order of
12 magnitude as bubble CH₄ release in Sallie's Fen (Goodrich et al., 2011). At that site the bubble
13 frequency of 35 ± 16 events m⁻² h⁻¹ was, however, lower than on the floating mat at Wyld
14 Lake Bog with 54 to 168 events m⁻² h⁻¹. In contrast to these findings, ebullition accounted on
15 average only for 20 % of fluxes at our bog site and 27 % in the pond (Figs. 3 and 5), where
16 bubble frequency of outer plots was less than 9 events m⁻² h⁻¹ and dropped to zero by the end
17 September (Fig. 3). In the pond ebullition was thus less important than reported previously in
18 11 lakes in Wisconsin (40 to 60 %; Bastviken et al., 2004) and two productive, urban ponds in
19 Sweden and China (> 90 %; Natchimuthu et al., 2014; Xiao et al., 2014).
20 Even though bubbles were rarely observed on p1, p2 and p3 farther away from the floating mat
21 (Fig. 7) and ceased altogether in September (Fig. 3), formation of CH₄ bubbles may have
22 initially been possible in the pond sediments. Concentrations exceeded the threshold
23 concentration of bubble formation at a N₂ partial pressure of 0.8 atm in all locations sampled
24 (Fig. 6). Such concentrations were only reached at larger sediment depth, though, and ongoing
25 stripping of N₂ with ebullition may have raised concentration thresholds over time (Fechner-
26 Levy and Hemond, 1996). At a remaining N₂ partial pressure of 0.5 atm, ebullition was not
27 possible from a theoretical point of view, which may explain its limited importance in the pond.
28 The lack of ebullition later on may have been assisted by falling temperatures in autumn; a
29 change from 20°C to 10°C, for example, raises the threshold for ebullition by 70 μmol L⁻¹. Flat
30 or linearly increasing concentration profiles near the sediment-water interface (Fig. 6) also
31 indicated a lack of active production of the gas in this zone. Concentrations of CH₄ and CO₂
32 remained low, typically less than 650 and 1500 μmol L⁻¹, respectively, suggesting that
33 microbial activity in the sediments was limited. Also the diffusive fluxes were small in units of
34 mass, about 3.5 mg CH₄-C m⁻² d⁻¹ and 7.5 mg CO₂-C m⁻² d⁻¹, respectively. The continuous
35 emission of CH₄ and CO₂ from the pond, on average 63 mg CH₄-C m⁻² d⁻¹ and 380 mg CO₂-C



1 $\text{m}^{-2} \text{d}^{-1}$, was hence likely driven by respiration in the water column and by advective inflow of
2 groundwater rich in CH_4 and CO_2 .
3 Our results further suggest that medium and infrequent large bubble events contributed a
4 substantial fraction to the total CH_4 flux at the floating mat but not in the bog and the pond (Fig.
5 8). This was the case even though small bubble events were much more frequent than large
6 ones (Fig. 8). DelSontro et al. (2015) also reported a strong positive correlation between
7 ebullition flux and bubble volume in open water and found that the largest 10 % of the bubbles
8 observed in Lake Wohlen, Switzerland, accounted for 65 % of the CH_4 transport. According to
9 the authors, large bubbles are disproportionately important because they contain exponentially
10 more CH_4 with increasing diameter, rise faster, and have less time and a relatively smaller
11 surface area to dissolve or exchange CH_4 with the surroundings (DelSontro et al., 2015).
12 The decline of CH_4 fluxes, CH_4 bubble frequency and contribution of ebullition from the
13 floating mat to the open water was striking and fluxes were also considerably higher than at the
14 peatland site (Fig. 7). These findings emphasize that the floating mats and transition zones to
15 the open water need to be included when quantifying greenhouse gas budgets of pond and
16 peatland ecosystems. We cannot mechanistically identify the causes for the observed pattern.
17 It seems likely that the peak emissions from the floating mat were caused by an optimum of
18 wet conditions in the peat favoring methanogenesis and impeding methane oxidation, presence
19 of some *Carex aquatilis* providing for conduit transport of the gas (Supplementary Information,
20 Table S1), and potentially by a release of methane from groundwater entering the land-water
21 interface. CH_4 flux through plants with aerenchymatic tissues can be responsible for 50 to 97 %
22 of the total CH_4 flux in peatlands because the aerenchyma link the anaerobic zone of CH_4
23 production with the atmosphere (Kelker and Chanton, 1997; Kutzbach et al., 2004; Shannon et
24 al., 1996). Kutzbach et al. (2004) found a strong positive correlation between the density of *C.*
25 *aquatilis* culms and CH_4 fluxes, as well as a contribution of 66 ± 20 % of the plant-mediated
26 CH_4 flux through *C. aquatilis* to the total flux in wet polygonal tundra. Since ebullition
27 dominated the CH_4 flux from the floating mat (Fig. 4) in our particular case this transport
28 mechanism seemed to be of more limited importance, though. Also recently fixed substrates
29 may have played a role for high CH_4 emissions from the floating mat. Several studies have
30 found a positive correlation between the rate of photosynthesis and CH_4 emissions (Joabsson
31 and Christensen, 2001; Ström et al., 2003), which has been explained by the quick allocation
32 of assimilated labile carbon to the roots and subsequent exudation to the anaerobic rhizosphere
33 (Dorodnikov et al., 2011). These recent photosynthates serve as a preferential source of CH_4
34 compared to older more recalcitrant organic matter (Chanton et al., 1995). Labile organic matter
35 produced by vascular plants was probably also imported from the floating mat to the margin of
36 the pond (Repo et al., 2007; Wik et al., 2013). Given the gradual decline of CH_4 fluxes along



1 the transect CH₄-rich groundwater may also have entered the floating mat and the pond, a
2 process that we did not investigate.

3

4 **4.2 Controls on CH₄ and CO₂ fluxes**

5 In agreement with earlier work air pressure change influenced methane flux. We observed 1.5-
6 to 3-fold higher CH₄ fluxes from the floating mat and the pond during periods of decreasing
7 compared to increasing air pressure (Fig. 9), which was very likely caused by increased
8 ebullition (Wik et al., 2013). Decreased atmospheric pressure results in bubble expansion,
9 which enhances buoyancy force and entails bubble rise (Chen and Slater, 2015).

10 The negative correlation of water and mat temperature with CH₄ and CO₂ fluxes from the pond
11 and CH₄ flux and ER of the floating mat (Table 1 and 2) was unexpected, as it is consensus that
12 temperature is an important positive control on these fluxes (Pelletier et al., 2014; Roulet et al.,
13 1997; Sachs et al., 2010; Wik et al., 2014). Also the potential effect of wind speed on CH₄ and
14 CO₂ fluxes from the pond was ambiguous. Increasing wind speeds should stimulate the
15 exchange of dissolved gases by increasing turbulence of both air and water close to the interface
16 (Crusius and Wanninkhof, 2003). Before August 15th, wind speed and CH₄ and CO₂ efflux from
17 the pond were, however, negatively correlated, whereas the correlation was positive thereafter
18 despite quite consistent wind speed patterns and surface water CO₂ concentrations throughout
19 the whole study period (Figs. 2 and S2, Supplementary Information).

20 Both phenomena may be explained by internal biological processes, i.e. the growth and decay
21 of a dense algal mat on the pond, changing hydrological connection between the pond system
22 and the surrounding peatland, and the influence of the vascular vegetation on the floating mat.
23 The algal mat developed in the beginning of July and was largely irreversibly dissolved by a
24 storm on August 12th (Figs. S4 and S5). During its presence CO₂ emissions from the pond
25 remained low (Fig. 3) and were overestimated by the boundary layer equation approach.
26 Amplitudes of dissolved CO₂ concentration were strong and concentration decreased with
27 increasing PAR (Table 1). Such dynamics reflects a strong autochthonous photosynthetic and
28 respiratory activity and lack of water mixing. The empirical relationship between CO₂
29 concentration gradient, wind speed and flux, which is largely controlled by turbulence in the
30 water column, obviously did not apply under such conditions. The subsequent shift to high CO₂
31 and CH₄ emissions was probably partly caused by the decomposition of the remains of the algal
32 mat, similarly as reported from a boreal and a subtropical pond (Hamilton et al., 1994; Xiao et
33 al., 2014). Other than that, the algal mat probably represented a physical barrier to diffusive and
34 ebullitive gas exchange between water column and atmosphere. We observed trapped gas
35 bubbles within the algal mat with CH₄ concentration of only 4 to 8 %; part of the originally
36 contained CH₄ may have been re-dissolved and oxidized. Even in shallow lakes and ponds, CO₂



1 and CH₄ concentrations can be several-fold higher in the deep water compared to the surface
2 water during certain periods (Dinsmore et al., 2009; Ford et al., 2002). We can only assume
3 that such concentration gradients established in or under the algal mat. Its destruction, mixing
4 of the water column and resuspension of the upper sediment layer probably entailed the
5 observed peak diffusive CO₂ and CH₄ emissions after the storm on August 12th (Fig. 2, Fig. 3).
6

7 **4.3 Relevance of greenhouse gas emissions from the pond system**

8 In terms of radiative forcing, the floating mat and open water behaved differently than the
9 peatland site during our daytime flux measurements at PAR > 1000 μmol m⁻² s⁻¹. All three bog
10 micro-sites represented daytime sinks of CO₂ equivalents and most so the hummocks (Fig. 10),
11 which represented about 90 % of the area. The floating mat and to a lesser extent also the pond
12 were sources of CO₂ equivalents to the atmosphere, even at daytime, and had a comparable
13 source strength as the boreal ponds and beaver pond investigated by Hamilton et al. (1994) and
14 Roulet et al. (1997). Net photosynthetic CO₂ uptake at light saturation was thus unable to
15 counterbalance the high CH₄ emissions of the floating mat in terms of CO₂ equivalents; at both
16 the floating mat and the pond emission of CH₄ was more important than CO₂ exchange in terms
17 of greenhouse gas equivalents. In the pond the average contribution of CH₄ was 59 %, which is
18 much higher than reported from a beaver pond at the Mer Bleue bog (5 %; Dinsmore et al.,
19 2009), but comparable to figures from ponds in other studies (36 to 91 %; Hamilton et al., 1994;
20 Huttunen et al., 2002; Pelletier et al., 2014; Repo et al., 2007; Roulet et al., 1997). We ascribe
21 the large differences between the floating mat and the peatland site (Figs. 7 and 10) to the influx
22 of allochthonous organic and inorganic carbon to the pond system from the surroundings and
23 to the different vegetation composition, in particular the occurrence of *Carex aquatilis* on the
24 floating mat, which may have enhanced CH₄ production and transport (Kutzbach et al., 2004;
25 Strack et al., 2006). Our results support earlier suggestions that ponds are important for the
26 greenhouse gas budget of peatlands at landscape scale (e.g. Pelletier et al. 2014) and they
27 suggest that changes in the area extent of floating mats and shore length will be an important
28 factor of changes in greenhouse gas budgets with predicted climate change.

29

30 **5 Conclusions**

31 Our summer measurements of atmospheric CH₄ and CO₂ exchange revealed a substantial small-
32 scale spatial variability with 6- and 42-fold increasing median CH₄ fluxes and bubble
33 frequencies, respectively, from the open water of the pond towards the surrounding floating
34 mat. Individual bubble events releasing more than 10 μmol CH₄ contributed substantially to
35 summer CH₄ emissions from the floating mat, despite their rare occurrence. When CH₄



1 emissions of peatlands that contain ponds are quantified, ebullitive and diffusive CH₄ fluxes at
2 the land-water interface hence need to be accounted for and the areal cover of the different
3 microforms and/or plant communities should be thoroughly mapped, as suggested by Sachs et
4 al. (2010) for tundra landscape. We also observed 4- to 16-fold increases in CH₄ and CO₂
5 emissions in late summer that were unrelated to meteorological drivers, such as temperature,
6 wind speed and radiation. Hydrological connections to adjacent peatlands and internal
7 hydrological and biological processes, such as the development of algal mats, which can be
8 abundant in small and shallow water bodies (e.g. Dinsmore et al., 2009; Hamilton et al., 1994;
9 Xiao et al., 2014) thus require more attention in the future. During our summer daytime flux
10 measurements, the pond system had a warming effect considering CH₄ and CO₂ exchange, with
11 the highest net release of CO₂ equivalents from the floating mat. We conclude that carbon
12 cycling and hydrology of small ponds and their surrounding ecotone need to be further
13 investigated; these systems are hot spots of greenhouse gas exchange and are likely highly
14 sensitive to anthropogenic climate change due to their shallowness and dependence on water
15 budgets and hydrological processes upstream.

16

17 **Acknowledgements**

18 The study was financially supported by the German Research Foundation (DFG) grant BL
19 563/21-1 and an international cooperation grant by the German Academic Exchange Service
20 (DAAD) to C. Blodau. We thank C. Wagner-Riddle for the possibility to use the former Blodau
21 laboratory at the School of Environmental Sciences at the University of Guelph and P. Smith
22 and L. Wing for organizational and technical support. We are grateful to M. Neumann from the
23 Grand River Conservation Authority for permission to conduct research in the Luther Marsh
24 Wildlife Management Area, Ontario, Canada, Z. Green for kindly providing satellite images of
25 the study area and C.A. Lacroix (OAC Herbarium, Biodiversity Institute of Ontario) for her
26 friendly help in identifying some plants. We are thankful to M. Goebel for support in the field
27 and advices on study design and data analysis and to Elisa Fleischer for her helpful comments.

28

29

30



References

- Bastviken, D., Cole, J.J., Pace, M.L., Tranvik, L.J.: Methane emissions from lakes: Dependence of lake characteristics, two regional assessments, and a global estimate. *Global Biogeochemical Cycles* 18, GB4009, 2004.
- Bastviken, D., Tranvik, L.J., Downing, J.A., Crill, P.M., Enrich-Prast, A.: Freshwater Methane Emissions Offset the Continental Carbon Sink. *Science* 331, 50, 2011.
- Bridgman, S.D., Cadillo-Quiroz, H., Keller, J.K., Zhuang, Q.: Methane emissions from wetlands: biogeochemical, microbial, and modeling perspectives from local to global scales. *Global Change Biology* 19, 1325–1346, 2013.
- Carmichael, M.J., Bernhardt, E.S., Bräuer, S.L., Smith, W.K.: The role of vegetation in methane flux to the atmosphere: should vegetation be included as a distinct category in the global methane budget? *Biogeochemistry* 119, 1–24, 2014.
- Chen, X., Slater, L.: Gas bubble transport and emissions for shallow peat from a northern peatland: The role of pressure changes and peat structure. *Water Resources Research* 51, 151–168, 2015.
- Ciais, P., Sabine, C., Bala, G., Bopp, L., Brovkin, V., Canadell, J., Chhabra, A., DeFries, R., Galloway, J., Heimann, M., Jones, C., Le Quéré, C., Myneni, R.B., Piao, S., Thornton, P.: Carbon and Other Biogeochemical Cycles, in: Stocker, T.F., Qin, D., Plattner, G.-K., Tignor, M., Allen, S.K., Boschung, J., Nauels, A., Xia, Y., Bex, V., Midgley, P.M. (Eds.), *Climate Change 2013: The Physical Science Basis. Contribution of Working Group I to the Fifth Assessment Report of the Intergovernmental Panel on Climate Change*. Cambridge, New York, pp. 465–570, 2013.
- Chanton, J.P., Bauer, J.E., Glaser, P.A., Siegel, D.I., Kelley, C.A., Tyler, S.C., Romanowicz, E.H., Lazrus, A.: Radiocarbon evidence for the substrates supporting methane formation within northern Minnesota peatlands. *Geochimica et Cosmochimica Acta* 59, 3663–3668, 1995.
- Cole, J.J., Prairie, Y.T., Caraco, N.F., McDowell, W.H., Tranvik, L.J., Striegl, R.G., Duarte, C.M., Kortelainen, P., Downing, J.A., Middelburg, J.J., Melack, J.: Plumbing the global carbon cycle: Integrating inland waters into the terrestrial carbon budget. *Ecosystems* 10, 171–184, 2007.



Crusius, J., Wanninkhof, R.: Gas transfer velocities measured at low wind speed over a lake. *Limnology and Oceanography* 48, 1010–1017, 2003.

Davidson, E.A., Savage, K., Verchot, L. V., Navarro, R.: Minimizing artifacts and biases in chamber-based measurements of soil respiration. *Agricultural and Forest Meteorology* 113, 21–37, 2002.

DelSontro, T., McGinnis, D.F., Wehrli, B., Ostrovsky, I.: Size Does Matter: Importance of Large Bubbles and Small-Scale Hot Spots for Methane Transport. *Environmental Science & Technology* 49, 1268–1276, 2015.

Dinsmore, K.J., Billett, M.F., Moore, T.R.: Transfer of carbon dioxide and methane through the soil-water-atmosphere system at Mer Bleue peatland, Canada. *Hydrological Processes* 23, 330–341, 2009.

Dinsmore, K.J., Billett, M.F., Skiba, U.M., Rees, R.M., Drewer, J., Helfter, C.: Role of the aquatic pathway in the carbon and greenhouse gas budgets of a peatland catchment. *Global Change Biology* 16, 2750–2762, 2010.

Dorodnikov, M., Knorr, K.H., Kuzyakov, Y., Wilmking, M.: Plant-mediated CH₄ transport and contribution of photosynthates to methanogenesis at a boreal mire: A ¹⁴C pulse-labeling study. *Biogeosciences* 8, 2365–2375, 2011.

Downing, J.A.: Emerging global role of small lakes and ponds: little things mean a lot. *Limnetica* 29, 9–24, 2010.

Downing, J.A., Cole, J.J., Middelburg, J.J., Striegl, R.G., Duarte, C.M., Kortelainen, P., Prairie, Y.T., Laube, K.A.: Sediment organic carbon burial in agriculturally eutrophic impoundments over the last century. *Global Biogeochemical Cycles* 22, GB1018, 2008.

Drösler, M.: Trace gas exchange and climatic relevance of bog ecosystems, Southern Germany. Doctoral thesis, Technical University of Munich, 2005.

Estop-Aragonés, C., Knorr, K.H., Blodau, C.: Controls on in situ oxygen and DIC dynamics in peats of a temperate fen. *Journal of Geophysical Research*, 117, 2012.

Fechner-Levy, E.J., Hemond, H.F.: Trapped methane volume and potential effects on methane ebullition in a northern peatland. *Limnology and Oceanography* 41, 1375–1383, 1996.



- Flessa, H., Rodionov, A., Guggenberger, G., Fuchs, H., Magdon, P., Shibistova, O., Zrazhevskaya, G., Mikheyeva, N., Kasansky, O., Blodau, C.: Landscape controls of CH₄ fluxes in a catchment of the forest tundra ecotone in northern Siberia. *Global Change Biology* 14, 2040–2056, 2008.
- Ford, P.W., Boon, P.I., Lee, K.: Methane and oxygen dynamics in a shallow floodplain lake: the significance of periodic stratification. *Hydrobiologia* 485, 97–110, 2002.
- Givelet, N., Roos-Barraclough, F., Shotyk, W.: Predominant anthropogenic sources and rates of atmospheric mercury accumulation in southern Ontario recorded by peat cores from three bogs: comparison with natural “background” values (past 8000 years). *Journal of Environmental Monitoring* 5, 935–949, 2003.
- Goodrich, J.P., Varner, R.K., Frohling, S., Duncan, B.N., Crill, P.M.: High-frequency measurements of methane ebullition over a growing season at a temperate peatland site. *Geophysical Research Letters* 38, L07404, 2011.
- Hamilton, J.D., Kelly, C.A., Rudd, J.W.M., Hesslein, R.H., Roulet, N.T.: Flux to the atmosphere of CH₄ and CO₂ from wetland ponds on the Hudson Bay lowlands (HBLs). *Journal of Geophysical Research* 99, 1495–1510, 1994.
- Hesslein, R.H.: An in situ sampler for close interval pore water studies. *Limnology and Oceanography* 21, 912–914, 1976.
- Huttunen, J.T., Väisänen, T.S., Heikkinen, M., Hellsten, S., Nykänen, H., Nenonen, O., Martikainen, P.J.: Exchange of CO₂, CH₄ and N₂O between the atmosphere and two northern boreal ponds with catchments dominated by peatlands or forests. *Plant and Soil* 242, 137–146, 2002.
- Joabsson, A., Christensen, T.R.: Methane emissions from wetlands and their relationship with vascular plants: an Arctic example. *Global Change Biology* 7, 919–932, 2001.
- Juutinen, S., Alm, J., Martikainen, P., Silvola, J.: Effects of spring flood and water level draw-down on methane dynamics in the littoral zone of boreal lakes. *Freshwater Biology* 46, 855–869, 2001.
- Juutinen, S., Rantakari, M., Kortelainen, P.L., Huttunen, J.T., Larmola, T., Alm, J., Silvola, J., Martikainen, P.J.: Methane dynamics in different boreal lake types. *Biogeosciences* 6, 209–223, 2009.



Juutinen, S., Väiranta, M., Kuutti, V., Laine, a. M., Virtanen, T., Seppä, H., Weckström, J., Tuittila, E.S.: Short-term and long-term carbon dynamics in a northern peatland-stream-lake continuum: A catchment approach. *Journal of Geophysical Research: Biogeosciences* 118, 171–183, 2013.

Kelker, D., Chanton, J.: The effect of clipping on methane emissions from *Carex*. *Biogeochemistry* 39, 37–44, 1997.

Kelly, C.A., Fee, E., Ramlal, P.S., Rudd, J.W.M., Hesslein, R.H., Anema, C., Schindler, E.U.: Natural variability of carbon dioxide and net epilimnetic production in the surface waters of boreal lakes of different sizes. *Limnology and Oceanography* 46, 1054–1064, 2001.

Kortelainen, P.L., Rantakari, M., Huttunen, J.T., Mattsson, T., Alm, J., Juutinen, S., Larmola, T., Silvola, J., Martikainen, P.J.: Sediment respiration and lake trophic state are important predictors of large CO₂ evasion from small boreal lakes. *Global Change Biology* 12, 1554–1567, 2006.

Kutzbach, L., Wagner, D., Pfeiffer, E.M.: Effect of microrelief and vegetation on methane emission from wet polygonal tundra, Lena Delta, Northern Siberia. *Biogeochemistry* 69, 341–362, 2004.

Larmola, T., Alm, J., Juutinen, S., Huttunen, J.T., Martikainen, P.J., Silvola, J.: Contribution of vegetated littoral zone to winter fluxes of carbon dioxide and methane from boreal lakes. *Journal of Geophysical Research: Atmospheres* 109, D19102, 2004.

Larmola, T., Bubier, J.L., Kobyljanec, C., Basiliko, N., Juutinen, S., Humphreys, E.R., Preston, M., Moore, T.R.: Vegetation feedbacks of nutrient addition lead to a weaker carbon sink in an ombrotrophic bog. *Global Change Biology* 19, 3729–3739, 2013.

Lerman A.: Chemical exchange across sediment-water interface. *Annual Review of Earth and Planetary Sciences* 6, 281–303, 1978.

Macrae, M.L., Bello, R.L., Molot, L.A.: Long-term carbon storage and hydrological control of CO₂ exchange in tundra ponds in the Hudson Bay Lowland. *Hydrological Processes* 18, 2051–2069, 2004.

McLaughlin, J., Webster, K.: Effects of Climate Change on Peatlands in the Far North of Ontario, Canada : A Synthesis. *Arctic, Antarctic and Alpine Research* 46, 84–102, 2014.

Michmerhuizen, C.M., Striegl, R.G., McDonald, M.E.: Potential methane emission from north-temperate lakes following ice melt. *Limnology and Oceanography* 41, 985–991, 1996.



Myhre, G., Shindell, D., Bréon, F.-M., Collins, W., Fuglestedt, J., Huang, J., Koch, D., Lamarque, J.-F., Lee, D., Mendoza, B., Nakajima, T., Robock, A., Stephens, G., Takemura, T., Zhang, H.: Anthropogenic and Natural Radiative Forcing, in: Stocker, T.F., Qin, D., Plattner, G.-K., Tignor, M., Allen, S.K., Boschung, J., Nauels, A., Xia, Y., Bex, V., Midgley, P.M. (Eds.), *Climate Change 2013: The Physical Science Basis. Contribution of Working Group I to the Fifth Assessment Report of the Intergovernmental Panel on Climate Change*. Cambridge, New York, pp. 659–740, 2013.

Natchimuthu, S., Panneer Selvam, B., Bastviken, D.: Influence of weather variables on methane and carbon dioxide flux from a shallow pond. *Biogeochemistry* 119, 403–413, 2014.

National Climate Data and Information Archive: Canadian Climate Normals. URL http://climate.weather.gc.ca/climate_normals/index_e.html (accessed November 18th, 2014).

Olefeldt, D., Turetsky, M.R., Crill P.M., McGuire, A.D.: Environmental and physical controls on northern terrestrial methane emissions across permafrost zones. *Global Change Biology* 19, 589–603, 2013.

Pelletier, L., Strachan, I.B., Garneau, M., Roulet, N.T.: Carbon release from boreal peatland open water pools: Implication for the contemporary C exchange. *Journal of Geophysical Research: Biogeosciences* 119, 207–222, 2014.

R Core Team: *R: A language and environment for statistical computing*. R Foundation for Statistical Computing, Vienna, 2014.

Raymond, P.A., Hartmann, J., Lauerwald, R., Sobek, S., McDonald, C., Hoover, M., Butman, D., Striegl, R.G., Mayorga, E., Humborg, C., Kortelainen, P.L., Dürr, H., Meybeck, M., Ciais, P., Guth, P.: Global carbon dioxide emissions from inland waters. *Nature* 503, 355–359, 2013.

Repo, M.E., Huttunen, J.T., Naumov, A. V., Chichulin, A. V., Lapshina, E.D., Bleuten, W., Martikainen, P.J.: Release of CO₂ and CH₄ from small wetland lakes in western Siberia. *Tellus* 59B, 788–796, 2007.

Roulet, N.T., Crill, P.M., Comer, N.T., Dove, A., Boubonniere, R.A.: Flux between a boreal beaver pond and the atmosphere. *Journal of Geophysical Research* 102, 29313–29319, 1997.



Sachs, T., Giebels, M., Boike, J., Kutzbach, L.: Environmental controls on CH₄ emission from polygonal tundra on the microsite scale in the Lena river delta, Siberia. *Global Change Biology* 16, 3096–3110, 2010.

Sander, R.: Compilation of Henry's Law Constants for Inorganic and Organic Species of Potential Importance in Environmental Chemistry. Max-Planck Institute of Chemistry, Mainz, 1999.

Sandilands, A.P.: Annotated Checklist of the Vascular Plants and Vertebrates of Luther Marsh, Ontario. *Ontario Field Biologist*, Special Publication No. 2. 1984.

Shannon, R.D., White, J.R., Lawson, J.E., Gilmour, B.S.: Methane efflux from emergent vegetation in peatlands. *Journal of Ecology* 84, 239–246, 1996.

Soumis, N., Canuel, R., Lucotte, M.: Evaluation of two current approaches for the measurement of carbon dioxide diffusive fluxes from lentic ecosystems. *Environmental Science and Technology* 42, 2964–2969, 2008.

Strack, M., Waller, M.F., Waddington, J.M.: Sedge succession and peatland methane dynamics: A potential feedback to climate change. *Ecosystems* 9, 278–287, 2006.

Ström, L., Ekberg, A., Mastepanov, M., Christensen, T.R.: The effect of vascular plants on carbon turnover and methane emissions from a tundra wetland. *Global Change Biology* 9, 1185–1192, 2003.

Sugimoto, A., Fujita, N.: Characteristics of methane emissions from different vegetations on a wetland. *Tellus* 49B, 382–392, 1997.

Tokida, T., Miyazaki, T., Mizoguchi, M., Nagata, O., Takakai, F., Kagemoto, A., Hatano, R.: Falling atmospheric pressure as a trigger for methane ebullition from peatland. *Global Biogeochemical Cycles* 21, GB2003, 2007.

Tranvik, L.J., Downing, J.A., Cotner, J.B., Loiselle, S.A., Striegl, R.G., Ballatore, T.J., Dillon, P., Finlay, K., Fortino, K., Knoll, L.B., Kortelainen, P.L., Kutser, T., Larsen, S., Laurion, I., Leech, D.M., McCallister, S.L., Mcknight, D.M., Melack, J.M., Overholt, E., Porter, J.A., Prairie, Y.T., Renwick, W.H., Roland, F., Sherman, B.S., Schindler, D.W., Sobek, S., Tremblay, A., Vanni, M.J., Verschoor, A.M., Wachenfeldt, E. Von, Weyhenmeyer, G.A.: Lakes and reservoirs as regulators of carbon cycling and climate. *Limnology and Oceanography* 54, 2298–2314, 2009.



- Trudeau, N.C., Garneau, M., Pelletier, L.: Methane fluxes from a patterned fen of the northeastern part of the La Grande river watershed, James Bay, Canada. *Biogeochemistry* 113, 409–422, 2013.
- Turunen, J., Tomppo, E., Tolonen, K., Reinikainen, A.: Estimating carbon accumulation rates of undrained mires in Finland – application to boreal and subarctic regions. *The Holocene* 12, 69–80, 2002.
- Varadharajan, C., Hemond, H.F.: Time-series analysis of high-resolution ebullition fluxes from a stratified, freshwater lake. *Journal of Geophysical Research: Biogeosciences* 117, G02004, 2012.
- Verpoorter, C., Kutser, T., Seekell, D.A., Tranvik, L.J.: A global inventory of lakes based on high-resolution satellite imagery. *Geophysical Research Letters* 41, 6396–6402, 2014.
- Walter, K.M., Zimov, S.A., Chanton, J.P., Verbyla, D., Chapin, F.S.: Methane bubbling from Siberian thaw lakes as a positive feedback to climate warming. *Nature* 443, 71–75, 2006.
- Wik, M., Crill, P.M., Varner, R.K., Bastviken, D.: Multiyear measurements of ebullitive methane flux from three subarctic lakes. *Journal of Geophysical Research: Biogeosciences* 118, 1307–1321, 2013.
- Wik, M., Thornton, B.F., Bastviken, D., MacIntyre, S., Varner, R.K., Crill, P.M.: Energy input is primary controller of methane bubbling in subarctic lakes. *Geophysical Research Letters* 41, 555–560, 2014.
- Xenopoulos, M.A., Lodge, D.M., Frentress, J., Kreps, T.A., Bridgham, S.D., Grossman, E., Jackson, C.J.: Regional comparisons of watershed determinants of dissolved organic carbon in temperate lakes from the Upper Great Lakes region and selected regions globally. *Limnology and Oceanography* 48, 2321–2334, 2003.
- Xiao, S., Yang, H., Liu, D., Zhang, C., Lei, D., Wang, Y., Peng, F., Li, Y., Wang, C., Li, X., Wu, G., Liu, L.: Gas transfer velocities of methane and carbon dioxide in a subtropical shallow pond. *Tellus* 66B, 23795, 2014.

Table 1. Correlations of CH₄ and CO₂ fluxes of the pond with environmental variables.

Flux	Time period	Spearman's rho	p	n
<i>mean air temperature since sunrise</i>				
CO ₂	whole period	- 0.54	< 0.001	147
CH ₄	whole period	- 0.36	< 0.001	147
diffusive CH ₄ ^a	whole period	- 0.67	< 0.001	119
<i>mean water temperature during measurements</i>				
CO ₂	whole period	- 0.47	< 0.001	94
CH ₄	whole period	- 0.50	< 0.001	94
diffusive CH ₄ ^a	whole period	- 0.60	< 0.001	82
<i>mean PAR of the last 3 h</i>				
CO ₂	whole period	- 0.49	< 0.001	147
<i>mean wind speed of the last 24 h</i>				
CO ₂	mid summer ^b	- 0.35	< 0.05	43
CO ₂	late summer ^c	+ 0.45	< 0.001	104
CO ₂	whole period	not significant		
CH ₄	mid summer ^b	- 0.35	< 0.05	43
CH ₄	late summer ^c	+ 0.63	< 0.001	104
CH ₄	whole period	+ 0.26	< 0.01	147
<i>maximum wind speed of the last 24 h</i>				
CO ₂	mid summer ^b	- 0.45	< 0.01	43
CO ₂	late summer ^c	+ 0.35	< 0.001	104
CO ₂	whole period	+ 0.17	< 0.05	147
CH ₄	mid summer ^b	- 0.55	< 0.001	43
CH ₄	late summer ^c	+ 0.63	< 0.001	104
CH ₄	whole period	+ 0.32	< 0.001	147

^a: only measurements without ebullition included

^b: July 10th to August 7th

^c: August 15th to September 29th

Table 2. Correlations of CH₄ and CO₂ fluxes of the floating mat with environmental variables.

Flux	Time period	Spearman's rho	p	n
<i>mean air temperature since sunrise</i>				
max. NEE	whole period	+ 0.74	< 0.001	20
CH ₄	whole period	- 0.42	< 0.001	79
<i>mean mat temperature during measurements</i>				
ER	whole period	- 0.44	< 0.01	38
CH ₄	whole period	- 0.41	< 0.001	79
diffusive	whole period	- 0.52	< 0.001	53
CH ₄ ^a				
<i>mean PAR during measurements</i>				
NEE	mid summer ^b	not significant		
NEE	late summer ^c	- 0.60	< 0.01	26
NEE	whole period	- 0.37	< 0.05	42

^a: only measurements without ebullition included

^b: July 10th to August 7th

^c: August 15th to September 29th



Figures

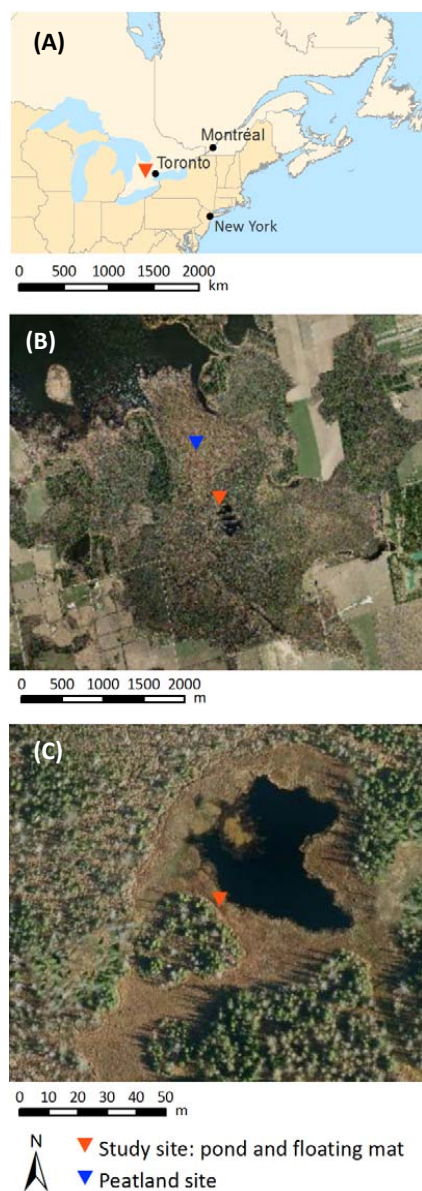


Figure 1. Location of the study site in southern Ontario, Canada (panel A), studied pond with floating mat and peatland site in Wylde Lake Bog in the Luther Marsh Wildlife Management Area with Luther Lake in the northwest (panel B) and close-up of the studied pond and floating mat (panel C) (Grand River Conservation Authority, 2010)

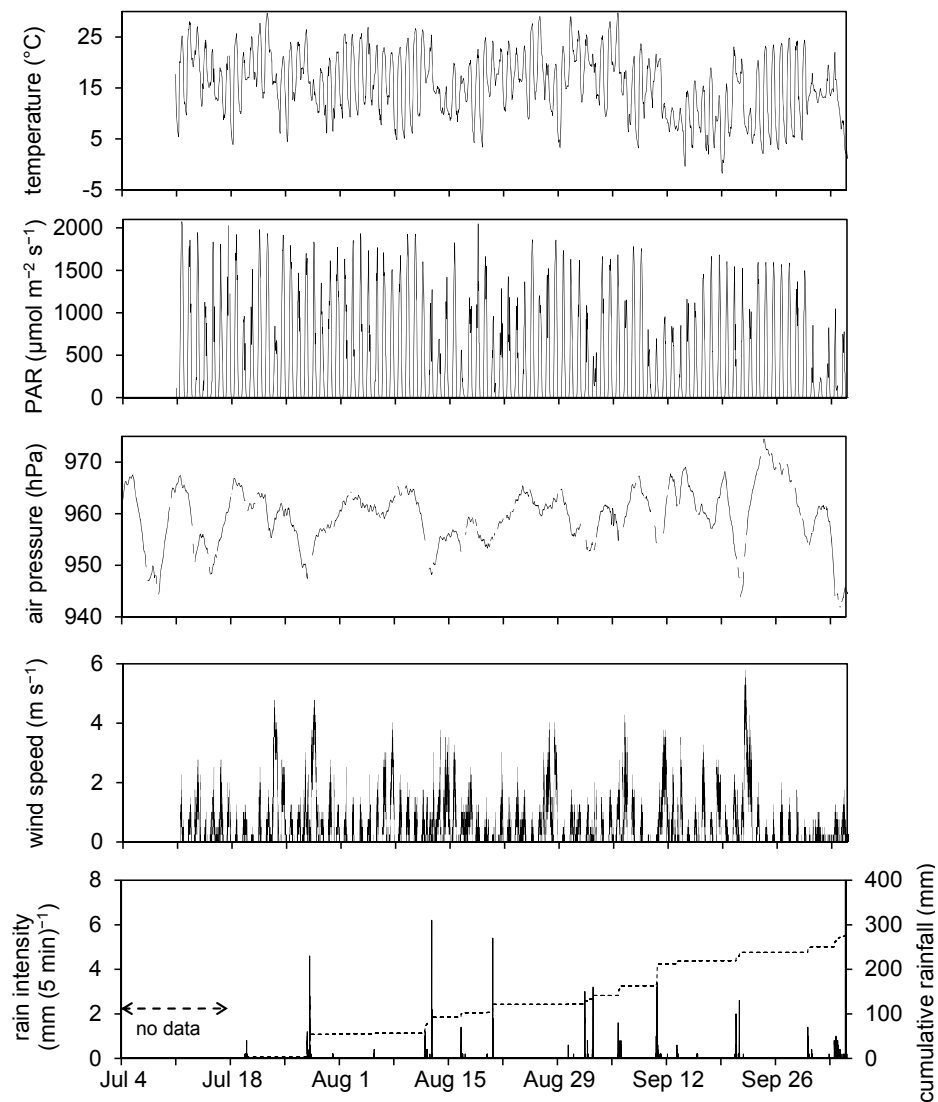


Figure 2. Time series of weather variables at the study site. Air temperature, photosynthetically active radiation (PAR) and air pressure are shown as hourly means, wind speed and rain intensity as 5 min averages. The dashed line in the lowest panel shows the cumulative rainfall.

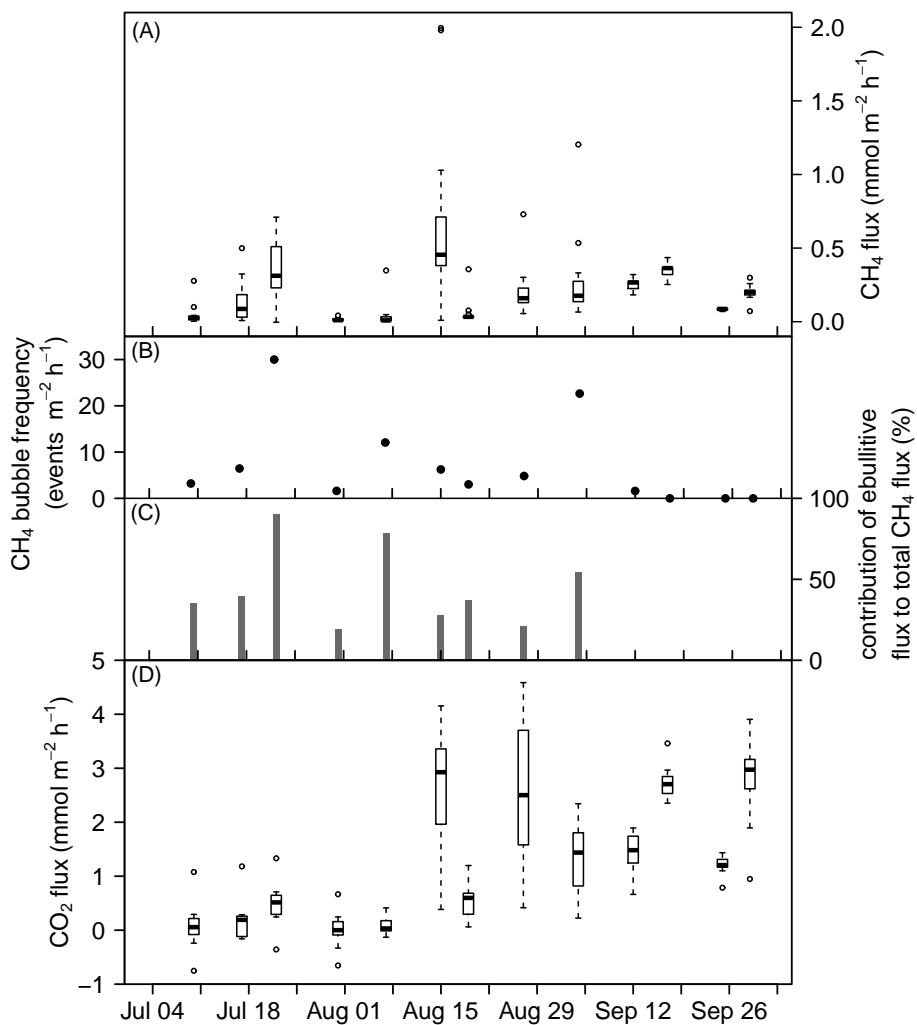


Figure 3. Time series of pond CH₄ fluxes (panel A), CH₄ bubble frequency (panel B), contribution of ebullitive CH₄ flux to total CH₄ flux (panel C) and CO₂ fluxes (panel D) on measuring days from July 10th until September 29th, 2014. In panel (A) and (D), the bold horizontal line shows the median, the bottom and the top of the box the 25th and 75th percentile and the whiskers include all values within 1.5 times the interquartile range.

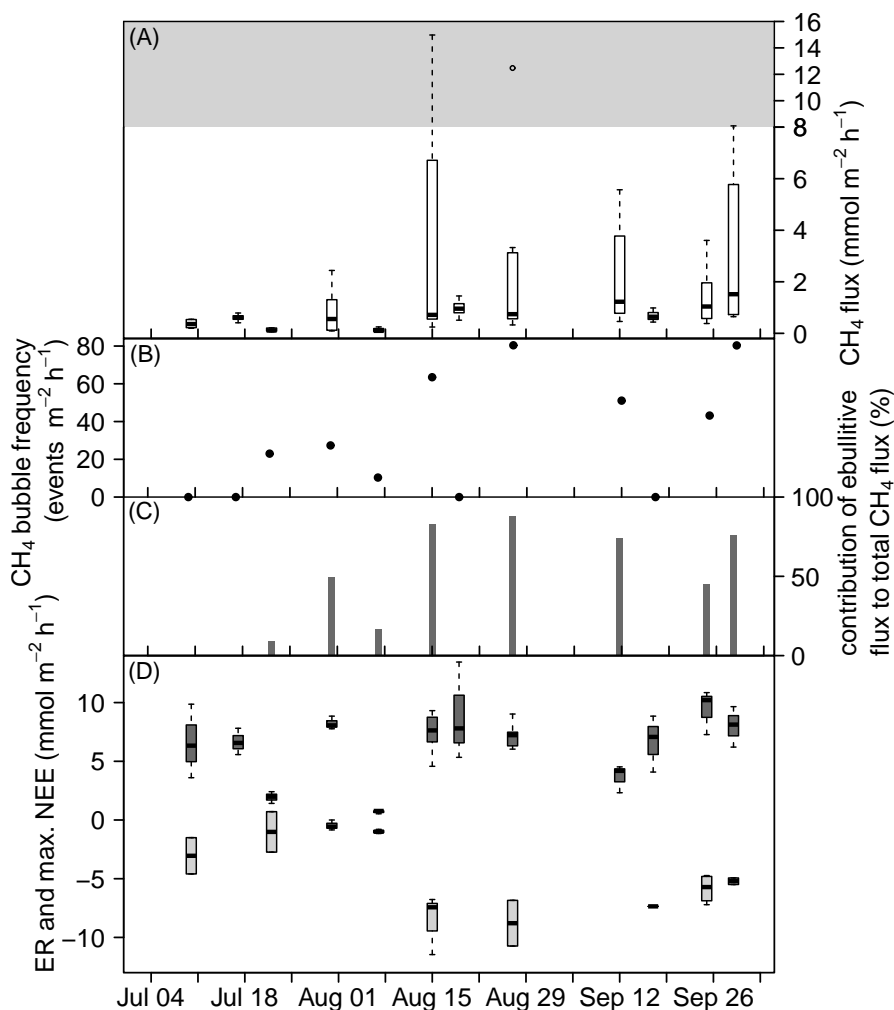


Figure 4. Time series of floating mat CH₄ fluxes (panel A), CH₄ bubble frequency (panel B), contribution of ebullitive CH₄ flux to total CH₄ flux (panel C) as well as ecosystem respiration (ER) and maximum net ecosystem exchange (NEE) (panel D) on measuring days from July 10th until September 29th, 2014. Note the different scaling of the y-axis within the gray area in panel (A). In panel (D), the dark gray boxes show the daytime ER and the light gray boxes the maximum net ecosystem exchange at values of photosynthetically active radiation > 1000 μmol m⁻² s⁻¹. In panel (A) and (D), the bold horizontal line shows the median, the bottom and the top of the box the 25th and 75th percentile and the whiskers include all values within 1.5 times the interquartile range.

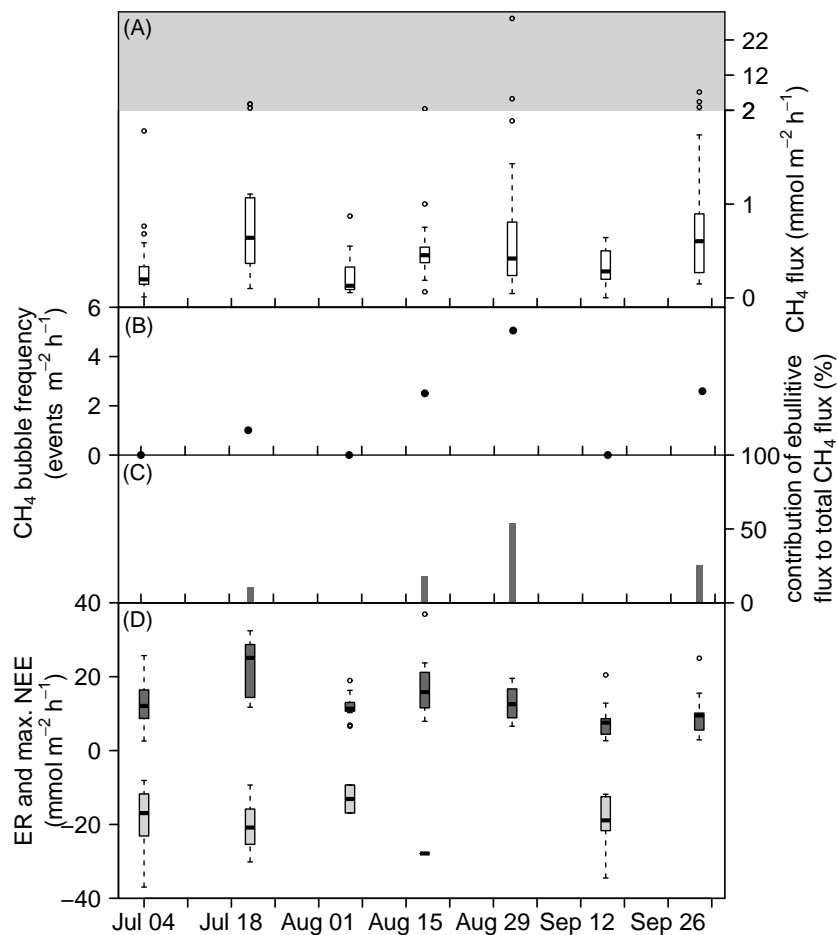


Figure 5: Time series of peatland CH₄ fluxes (panel A), CH₄ bubble frequency (panel B), contribution of ebullitive CH₄ flux to total CH₄ flux (panel C) as well as ecosystem respiration (ER) and maximum net ecosystem exchange (NEE) (panel D) on measuring days from July 4th until October 1st, 2014. Note the different scaling of the y-axis within the gray area in panel (A). In panel (D), the dark gray boxes show the daytime ER and the light gray boxes the maximum net ecosystem exchange at values of photosynthetically active radiation > 1000 $\mu\text{mol m}^{-2} \text{s}^{-1}$. In panel (A) and (D), the bold horizontal line shows the median, the bottom and the top of the box the 25th and 75th percentile and the whiskers include all values within 1.5 times the interquartile range.

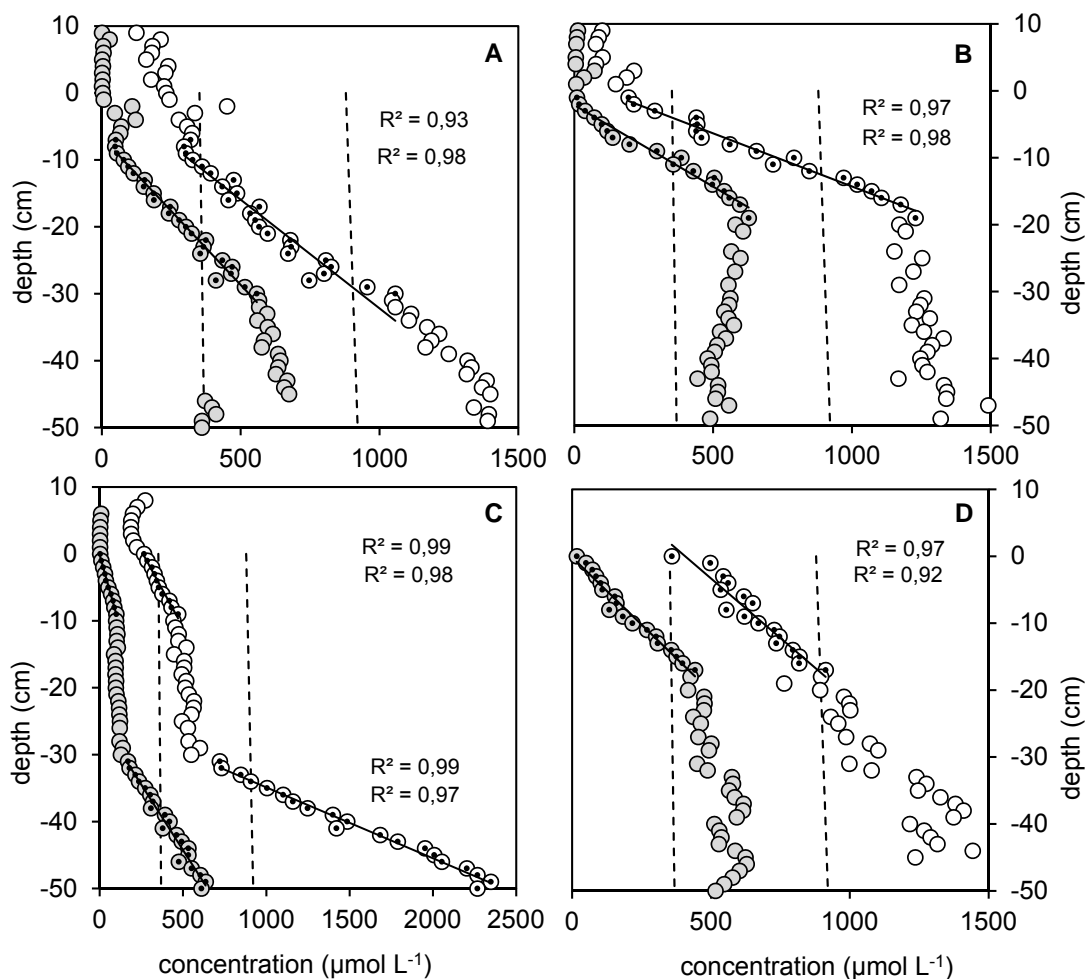


Figure 6: CH_4 (shaded symbols) and CO_2 (open symbols) concentrations near the sediment-water interface and in the sediment of the pond in four locations (A – D) on September 25th and 29th, respectively. Black lines represent regression slopes (with regression coefficient R^2) used to calculate diffusive fluxes towards the sediment-water interface. Dashed lines denote depth and temperature dependent theoretical thresholds for formation of CH_4 bubbles at 0.8 atm (lower line) and 0.5 atm (upper line) partial pressure of N_2 in the pond sediment at 15°C. In panel C also the diffusive flow from deeper



sediment layers was calculated.

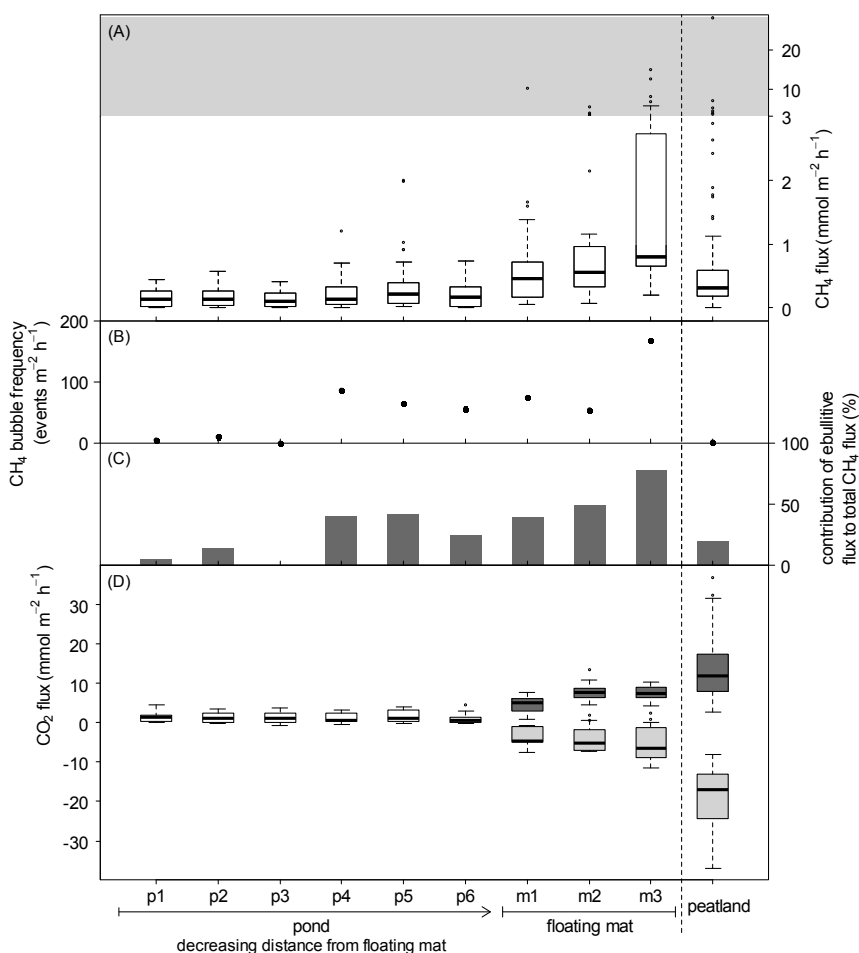


Figure 7: CH₄ fluxes (panel A), CH₄ bubble frequency (panel B), contribution of ebullitive CH₄ flux to total CH₄ flux (panel C) and CO₂ fluxes (panel D) of the pond (p1 to p6) along a gradient of decreasing distance from the floating mat, of the 3 measuring plots on the floating mat (m1 to m3) and of the peatland site for comparison. Note the different scaling of the y-axis within the gray area in panel (A). In panel (D), the transparent boxes show the net CO₂ flux of the pond, the dark gray boxes the daytime ER and the light gray boxes the maximum net ecosystem exchange of the floating mat and the peatland at values of photosynthetically active radiation > 1000 $\mu\text{mol m}^{-2} \text{s}^{-1}$. In panel (A) and (D), the bold horizontal line shows the median, the bottom and the top of the box the 25th and 75th percentile and the



whiskers include all values within 1.5 times the interquartile range.

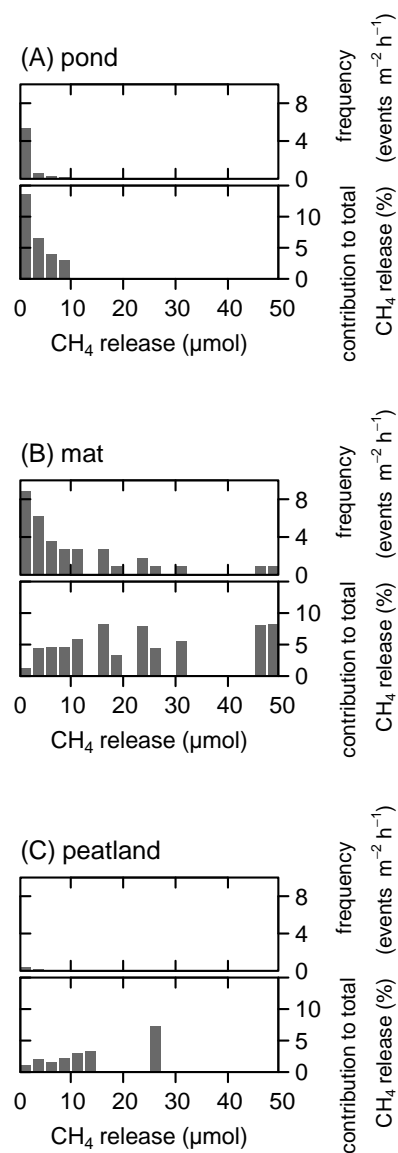


Figure 8: Frequency distribution of ebullitive CH₄ release (upper panels) as well as contribution of each size group of ebullitive CH₄ release to the total CH₄ release (lower panels) of the pond (panel A), the floating mat (panel B) and the peatland (panel C).

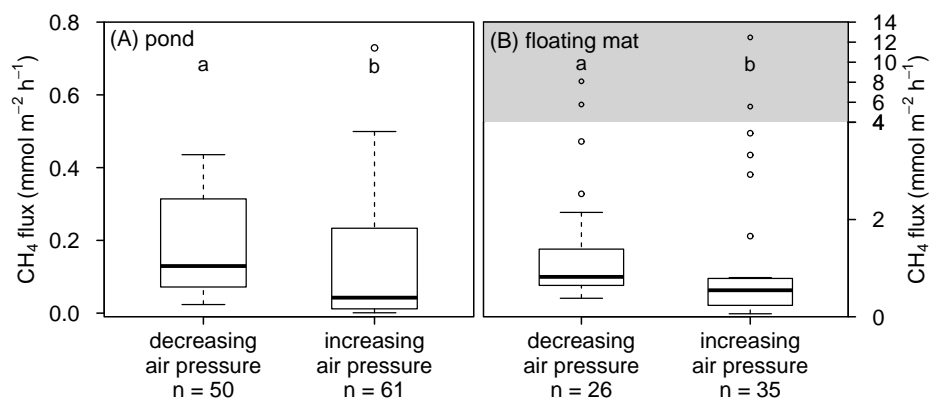


Figure 9: CH₄ fluxes during decreasing and an increasing air pressure trends over the last 24 h for the pond (panel A) and the floating mat (panel B). Different letters indicate significant differences (Kruskal-Wallis test, $p < 0.05$ and $p < 0.01$, $n = 111$ and $n = 61$). Note the different scaling of the y-axis within the gray area in panel (B). The bold horizontal line shows the median, the bottom and the top of the box the 25th and 75th percentile and the whiskers include all values within 1.5 times the interquartile range.

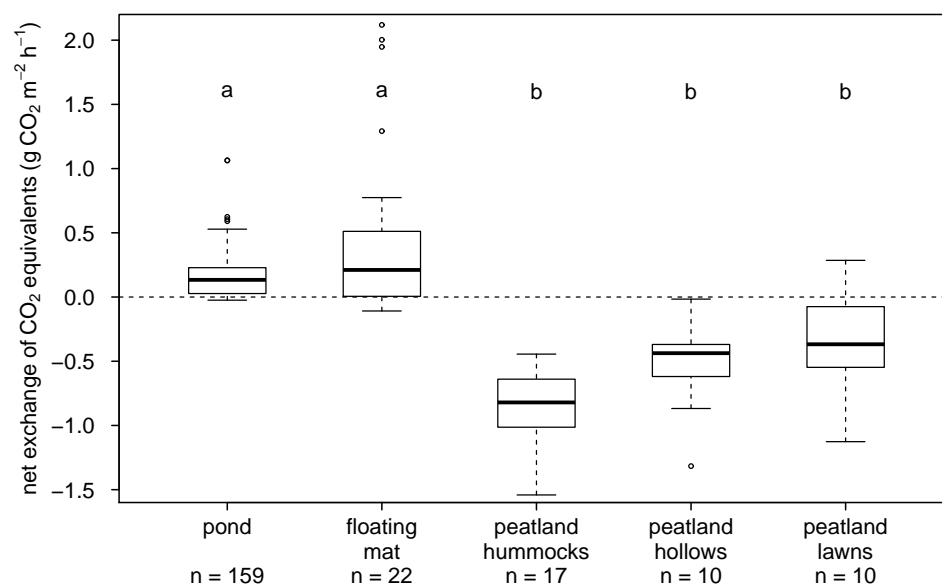


Figure 10: Daytime net exchange of CO₂ equivalents of the pond, the floating mat and the three different microforms of the peatland. Different letters indicate significant differences (Kruskal-Wallis multiple comparison test, $p < 0.001$, $n = 218$). For comparability of the CO₂ fluxes of the floating mat and the peatland, only maximum net ecosystem exchange at values of photosynthetically active radiation $> 1000 \mu\text{mol m}^{-2} \text{s}^{-1}$ was used for the calculation. The bold horizontal line shows the median, the bottom and the top of the box the 25th and 75th percentile and the whiskers include all values within 1.5 times the interquartile range.